

Environmental heterogeneity patterns plant species richness and turnover in two hyperdiverse floras

Running title: Environmental heterogeneity and plant species richness

Ruan van Mazijk, Michael D. Cramer & G. Anthony Verboom

Department of Biological Sciences, University of Cape Town, Rondebosch, South Africa

Corresponding author: RVM (ruanvmazijk@gmail.com, +27 21 650 3684)

ORCID nos.: RVM: 0000-0003-2659-6909, MDC: 0000-0003-0989-3266, GAV: 0000-0002-1363-9781

Abstract

****Aim:****

Location: The Greater Cape Floristic Region in southwest Africa (the Cape), and the Southwest Australia Floristic Region (SWA)

Taxon: Vascular plants

Methods: Geospatially explicit floral and environmental data, non-parametric statistics, boosted regression tree modelling

Results: The Cape is more environmentally heterogeneous and has higher levels of floristic turnover than SWA. We find that environmental heterogeneity is the main predictor of species richness in the Cape, and somewhat less so for SWA. Edaphic conditions are found to be of more biologically important in the Cape, though this is contingent on the quality of the data modelled.

Main conclusions:

Keywords: biodiversity, environmental heterogeneity, fynbos, Greater Cape Floristic Region, kwongan,

14 macroecology, species richness, species turnover, vascular plants, Southwest Australia Floristic Region

15 **Acknowledgements**

16 This work was funded by the South African Department of Science and Technology (DST) and the National
17 Research Foundation (NRF) under the DST-NRF Innovation Honours Scholarship (to RVM), and by the South
18 African Association of Botanists (SAAB) Honours Scholarship (to RVM). Thanks go to the Department of
19 Biological Sciences, University of Cape Town, for providing a 2TB external hard drive for local GIS data
20 storage. Many computations were performed using facilities provided by the University of Cape Town's ICTS
21 High Performance Computing team (hpc.uct.ac.za).

22 **1 Introduction**

23 Biodiversity represents the variety of species and the ecological and evolutionary processes that bring about
24 those species (???; Bohn & Amundsen, 2004). Studying the distribution of biodiversity in space is a major
25 avenue of biological research (???; Kreft & Jetz, 2007). Regional-scale geographic patterns in species richness
26 have long been studied, particularly in biodiversity hotspots (???; Cook et al., 2015). The spatial distribution of
27 species richness can be explained in terms of the physical environment. Properties of the environment have
28 been suggested to influence species richness in three ways: (i) resources and energy, which can determine the
29 number of species able to co-exist in an area (Gaston, 2000; Kreft & Jetz, 2007; Mouchet et al., 2015); (ii)
30 stability through time, which enables species' persistence; and (iii) spatial heterogeneity, which can stimulate
31 ecological speciation and possible barriers to gene flow and can facilitate greater levels of species' co-existence
32 (Thuiller et al., 2006; Mouchet et al., 2015; Cramer & Verboom, 2016). The physical environment, then, can be
33 used to explain species richness in both a local-deterministic and historical sense (Ricklefs, 1987).

34 The maintenance of species richness, particularly the coexistence of high numbers of species in biodiversity
35 hotspots, is often regarded as “paradoxical” (Hart et al., 2017), and is a central problem in ecology (Ricklefs,
36 1987; Kreft & Jetz, 2007; Hart et al., 2017). Species richness is constrained by the ability of habitats to support
37 a variety of species—its ecological carrying capacity (Mateo et al., 2017). This is exemplified in modelling
38 approaches, wherein species richness is a function of environmental predictors in a correlative framework
39 (“macro-ecological models”; Mateo et al., 2017). Macroecological models of species richness implicitly

40 assume that communities are saturated, following species-area and species-energy relationships, and at
41 equilibrium with the environment (Mateo et al., 2017).

42 A solution to the “paradox” of species co-existence is environmental heterogeneity (EH): a more heterogeneous
43 environment gives rise to a larger environmental space, and can thus facilitate co-existence between more
44 species, generating more diverse species assemblages. Heterogeneity in the physical environment is known to
45 be positively associated with species richness (Rensburg et al., 2002; Hart et al., 2017), and has been
46 demonstrated to do so across many taxa—e.g. Canadian butterflies (???), European vertebrates (Mouchet et al.,
47 2015), South African birds (Rensburg et al., 2002), in communities along marine continental margins (Levin et
48 al., 2010), French scarab beetles (Lobo et al., 2004), and for global terrestrial plants (Kreft & Jetz, 2007). The
49 spatial scale of heterogeneity, or “grain” of the environment, is also important to consider (Hart et al., 2017), as
50 spatial scale in absolute environmental conditions has also been explored (???; Baudena et al., 2015; Mouchet
51 et al., 2015). Species co-existence and biodiversity maintenance is indeed suggested to be scale-dependent
52 (Hart et al., 2017).

53 EH is often under-represented in macro-ecological models of species richness, and has recently been found to
54 explain up to ca. 95% of biome level species richness across South Africa (Cramer & Verboom, 2016). Indeed,
55 models that include EH yield better estimates of the richness of the Cape flora (Thuiller et al., 2006; Cramer &
56 Verboom, 2016). Mediterranean-type terrestrial biodiversity hotspots, such as the Cape flora included in the
57 models by Cramer & Verboom (2016), present interesting study systems in which to investigate the relationship
58 between the environment and species richness. These systems exhibit far greater species richness than
59 predicted by their areas, productivities and latitudes (Cowling et al., 1996; Kreft & Jetz, 2007). There are five
60 Mediterranean biodiversity hotspots on Earth: the California Floristic Province, the Mediterranean Basin, the
61 Chilean Winter Rainfall-Valdivian Forests, the Greater Cape Floristic Region, and the Southwest Australia
62 Floristic Region (Cowling et al., 1996; Hopper & Gioia, 2004; Cook et al., 2015). These ecosystems have
63 regular fire-cycles (Cowling et al., 1996), climatic buffering, and long term stability (Kreft & Jetz, 2007),
64 shrubby, sclerophyllous flora (Hopper & Gioia, 2004). Together, they account for ca. 20% of global vascular
65 plant species, yet only ca. 5% of global land surface areas (Cowling et al., 1996). Various hypotheses have
66 been proposed to explain the high levels of plant species richness in these regions (Cook et al., 2015). The
67 species accumulation hypothesis states that the stability of these regions has allowed many species to accrue.
68 The species co-existence hypothesis states that these hotspots may facilitate greater degrees of species
69 co-existence in smaller spatial areas, due to fine-scale heterogeneity in their environments. Indeed, EH has
70 evolutionary implications too, stimulating ecological speciation across sharp environmental gradients.

71 Both the Southwest Australia Floristic Region (SWA) and the Greater Cape Floristic Region (Cape) are
72 Mediterranean-type biodiversity hotspots, particularly in terms of plant species. Where the Cape (with an area
73 of ca. 189,000 km²) is known to contain about 11,400 plant species (about 0.060 species per km²), SWA (area
74 of ca. 270,000 km²) has about 3,700 species (0.014 species per km²) (???). So, the Cape has ca. 4.3 times as
75 many species per km² as SWA. The Cape and SWA are appropriately often compared, due to the similarities
76 between their environments (e.g. oligotrophic soils, an oceanically buffered moderate climate) and their plants'
77 ecologies (Hopper & Gioia, 2004). These two regions present unique flora out of the five Mediterranean
78 systems, with high levels of endemism (Cowling et al., 1996), and many obligate fire-adapted species (Cowling
79 et al., 1996). Similarities withstanding, SWA is topographically and edaphically distinct from the Cape. The
80 former is topographically rather uniform (i.e. flat)—uniquely so among the world's five Mediterranean-climate
81 regions (Hopper & Gioia, 2004)). SWA possesses a mesoscale chronosequence dune system (Laliberte et al.,
82 2014; Cook et al., 2015), while the Cape is mountainous, topographically heterogeneous, and therefore
83 associated with a large degree of spatial climatic variability, with a fine-scale mosaic of geologies and soils
84 (Cowling et al., 1996; Cramer et al., 2014; Verboom et al., 2017).

85 Both regions have sources of edaphic heterogeneity, but at different scales. This edaphic variability may aid in
86 explaining the species richness in these regions (Beard et al., 2000; Verboom et al., 2017). EH of many forms
87 will likely be important in macro-ecological models in both regions, as both regions have been relatively
88 environmentally stable over evolutionary time-scales (Wardell-Johnson & Horwitz, 1996; Hopper & Gioia,
89 2004; Lambers et al., 2010; Cramer et al., 2014; Laliberte et al., 2014; Cook et al., 2015). For the Cape, high
90 levels of species richness are thought to result from long term climatic stability, and fine grain variation in
91 geology and soils (Cramer et al., 2014). The question thus arises whether heterogeneity is a significant
92 contributor to SWA species richness. In the absence of topographic variability in SWA, it is proposed that the
93 heterogeneity of that region is due to the juxtaposition of soil types (Laliberte et al., 2014; Cook et al., 2015),
94 creating extreme edaphic variation.

95 Our hypotheses concern the Cape and SWA's environments and floras. Our main hypothesis is that the Cape
96 possesses greater abiotic heterogeneity, and at finer grain, compared to SWA, such as to explain the Cape's
97 greater species richness per unit area, and proposed greater levels of species turnover between areas. We also
98 conjecture that the heterogeneity that predicts species richness in SWA will be more pronounced in terms of
99 edaphic variables. Here we attempt to assess five key predictions of this hypothesis, additionally investigating
100 a seventh prediction to test the conjectured role of edaphic heterogeneity in SWA. Dealing with the two
101 regions' environments, we assess (i) whether the Cape environment is more heterogeneous than that of SWA

102 and (ii) whether the Cape environment has more pronounced heterogeneity at finer scales than that of SWA.
103 Dealing with the distribution of species in the two regions, we assess (iii) whether the Cape exhibits greater
104 levels of species turnover between areas. Relating each regions' environment and flora, we finally assess (iv)
105 whether species richness and species turnover are adequately predicted by EH in both regions and whether (v)
106 species richness and species turnover are better predicted by different forms of EH in either region (e.g. the
107 importance of edaphic heterogeneity in SWA).

108 **2 Materials and methods**

109 **2.1 Overview**

110 Our analyses defined boundaries for each region, those regions' environmental data and geospatially-explicit
111 vascular plant occurrence records, all based on publicly available data. The environmental variables chosen
112 (Table 1) for this study were intended to cover a reasonable spread of climatic, edaphic, and ecologically
113 relevant environmental axes, and are not intended to be exhaustive. We selected variables describing
114 topography (elevation), productivity (NDVI), soil status and climate and climatic seasonality.

115 We carried out this investigation at four principal spatial scales: 0.05° x 0.05° squares (the finest common
116 resolution among the environmental data sources used), quarter degree squares (QDS) (Larsen et al., 2009),
117 half degree squares (HDS) (Larsen et al., 2009) and three-quarter degree squares (3QDS). For the Cape, most
118 plant occurrence records are only accurate to QDS level. Thus, analyses involving species occurrence data were
119 necessary limited to scales including and above QDS.

120 Analyses were performed in R v3.4.0–3.5.1 (R Core Team, 2018). Version-numbers of specific R packages
121 used are presented in the bibliography.

122 **2.2 Environmental data sources**

123 The GCFR was treated as the areas occupied by the Succulent Karoo and Fynbos biomes in the current
124 delineation of South Africa's biome boundaries (Mucina & Rutherford, 2006). The SWAFR was treated as the
125 areas occupied by the Southwest Australia savanna, Swan Coastal Plain Scrub and Woodlands, Jarrah-Karri
126 forest and shrublands, Southwest Australia woodlands, Esperance mallee, and Coolgardie woodlands in the

World Wildlife Fund Terrestrial Ecoregions dataset (Olson et al., 2001) in order to closely match the currently delineated SWAFR (Gioia & Hopper, 2017, Hopper & Gioia (2004)). For the sake of readability, we shall refer to the GCFR and SWAFR simply as the Cape and SWA from hereon.

Geospatially-explicit raster layers were acquired for a selection of environmental variables (Table 1), for the regions of interest. Raster data were re-projected to a common coordinate reference: WGS84 (NIMA, 2000), using the “rgdal” (???) package in R (R Core Team, 2018). All data were re-sampled to 0.05° resolution using the “resample” function in the R package “raster” (???), with the “bilinear” method.

An emphasis was made on using satellite-derived environmental data in this work, in order to minimise differences in data quality and methodologies between the Cape and SWA. Additionally, satellite-derived data have been shown to benefit regional-scale species distribution models (Deblauwe et al., 2016), thus motivating their use in this regional-scale study. The environmental data used in this study were derived from NASA’s SRTM digital elevation model (Farr et al., 2007), NASA’s MODIS/Terra spectroradiometric data for land surface temperature and NDVI, the Climate Hazards Group’s CHIRPS rainfall dataset (Funk et al., 2015), and the International Soil Reference and Information Centre’s SoilGrids250m edaphic dataset (Hengl et al., 2017) (Table 1). SRTM and MODIS are entirely derived from satellite measurements, whereas CHIRPS is interpolated from weather station data with satellite-derived radiometric measurements. SoilGrids250m is a machine-learning derived product, based on soil measurements as a function of many covariates, including MODIS and STRM sources (see Hengl et al., 2017), using random-forests and other classification-tree-based methods, including gradient-boosting. For the soil data considered here (Table 1), we used depth-interval weighted average values as the value for a particular soil variable in a given place.

Climatic and spectral data arise from satellites monitoring properties of the Earth’s surface through time. We therefore use the mean annual values for rainfall, surface temperature, and NDVI in each pixel in our analyses. Pronounced seasonality of rainfall is a known feature of mediterranean systems (???). We describe this seasonality by computing computing the precipitation in the driest quarter (PDQ), using methods based on the “biovars” function in the R package “dismo”.

2.3 Plant occurrence data

Geospatially-explicit records of vascular plant occurrences were downloaded from the Global Biodiversity Information Facility (GBIF, Table 1). Queries were made for tracheophyte records from within the borders of

155 the Cape and SWA as treated here (GBIF, 24 July 2017, GBIF (24 July 2017)). Only records with defined
 156 species and intra-specific ranks were kept. Intra-specific occurrences were treated as simply being
 157 representative of their species. This resulted in FIXME unique species names in the Cape, and FIXME in SWA.

158 We cleaned these data using the R package “taxise” (???, (???)) to check that these species names had
 159 accepted-status among taxonomic databases. We queried two major taxonomic databases: the Global Name
 160 Resolver (GNR), and the Taxonomic Name Resolution Service (TNRS). Should either one of these services
 161 return at least one match for a given name, then that name was accepted. Those names for which no full
 162 binomial matches were found in either database were excluded from the final list of species. The number of
 163 species names excluded totalled at FIXME and FIXME for the Cape and SWA respectively. Especially for
 164 SWA, these numbers may be deemed appreciably high. But, the occurrence records that would be dropped, as a
 165 consequence of these names’ removals, appeared randomly distributed in geographic space in both regions. As
 166 such, any effect of the loss of these records in this analysis is likely uniform within the two regions.

167 After the unaccepted names were removed, it was important to ensure that a species was not listed under
 168 multiple synonyms. Such cases would skew estimates of species richness and turnover in this study. In light of
 169 this, the remaining names were queried in the Tropicos and Integrated Taxonomic Information System (ITIS)
 170 databases for their known synonyms, again using “taxize”. These were collated to produce a nomenclatural
 171 “thesaurus” for the Cape and SWA species. This consisted of a list of the accepted species names in a region,
 172 each associated with a list of known synonyms. We amended species’ names in the GBIF occurrence data, in
 173 order ensure species were listed under only one of these synonyms, replacing all appearances of a species’
 174 synonyms with the first synonym used in the list.

175 Lastly, We removed any species from both regions that are invasive aliens or non-indigenous. Alien species
 176 lists for plants in South Africa and Australia were acquired from the IUCN’s Global Invasive Species Database
 177 (<http://www.iucngisd.org/gisd/>).

178 The final total plant species richness in each region was FIXME and FIXME for the Cape and SWA
 179 respectively. These final collections of species occurrence records were converted to raster-layers, wherein
 180 pixel-values represented the species richness of vascular plants within that pixel. These rasters were produced
 181 at QDS, HDS, and 3QDS resolutions.

182 2.4 Analyses

183 2.4.1 Quantifying environmental heterogeneity

184 In order to assess predictions (i) and (ii), we needed to describe the EH in both regions. Using the R package
185 “raster” (???), we used a modified version of the “roughness” index in the “terrain” function. For a three by
186 three neighbourhood \mathbf{N} of cells, our index of roughness R is the average square-root of the squared difference
187 between each of the n neighbour cells’ values x_i and the central focal cell’s value x_{focal} :

$$R(\mathbf{N}) = \frac{1}{n} \sqrt{\sum_{i=1}^n (x_{\text{focal}} - x_i)^2} \quad (1)$$

188 This value, notionally equivalent to the standard deviation of values relative to the focal value, is ascribed to
189 the focal cell. Note, in order to use as much data from within regions’ borders as possible, roughness was
190 computed if a focal cell had at least one neighbour cell. Using this index, we produced raster layers of each of
191 our nine environmental variable’s heterogeneity. We compared the distributions of “roughness” values in each
192 variable in each region with non-parametric Mann-Whitney U -tests, as almost all variables were highly
193 non-normal, and could not be normalised by log-transformations. We also compare the effect size of the Cape
194 vs SWA using the “common language effect size” ($CLES$), using the R package “canprot”. The $CLES$ is the
195 proportion of all pairwise comparisons between two sample groups’ observations where one group’s value is
196 greater than the other’s. We calculated the $CLES$ as the proportion of pairs where Cape roughness values
197 were greater than that of SWA. This allowed us to assess prediction (i). To compare the spatial scales of
198 heterogeneity (prediction (ii)) between each region, we repeated this analysis at all four spatial scales. This
199 entailed recalculating the roughness layer for each variable after the original layer (0.05 degrees resolution) had
200 been rescaled to each of the coarser resolutions.

201 2.4.2 Quantifying species turnover

202 Regarding prediction (iii), we wished to compare the general degree of species turnover in each region. To
203 compare the extent of species turnover between the Cape and SWA, we determined two metrics of species
204 turnover. The first, computes the mean species turnover as Jaccard distances (???) between each pair of QDS
205 within each HDS (\bar{J}_{QDS} , based on HDS with $2 \leq n \leq 4$ QDS) in both regions. The second is defined in terms
206 of Whittaker’s additive definition of β -diversity (???), as follows:

$$\gamma = \alpha + \beta \quad (2)$$

Here, we treat species richness at the HDS-scale (S_{HDS}) as γ -diversity and at the QDS-scale (\bar{S}_{QDS}) as α -diversity. Intuitively, the species richness of an area is the result of some combination of the richness of sites within that area and the difference in species complements between those sites. Thus, we partition γ -diversity as in Equation (2), such that β -diversity is the difference between γ - and α -diversity. We compare the distributions of \bar{J}_{QDS} and T_{HDS} using non-parametric Mann-Whitney U -tests, in order to guard against non-normality.

2.4.3 Predicting richness and turnover with environmental heterogeneity

Regarding prediction (iii), we wished to compare the general degree of species turnover in each region. For (iv) and (v) we modelled species richness (S) and turnover as a function of various combinations of environmental and environmental heterogeneity variables in both regions using boosted regression-tree (BRT) modelling techniques. This allowed us to explore which axes of environmental heterogeneity are most influential on vascular plant species richness and turnover, and the differences in the importance of such axes between the Cape and SWA.

BRTs are a flexible machine learning-based model of response variables and do so without involving normal null-hypothesis significance testing (Elith et al., 2008), and have been employed previously to model species richness (Thuiller et al., 2006; see Mouchet et al., 2015; Cramer & Verboom, 2016) as macro-ecological models. BRTs are developed through the iterative generation of non-linear regression trees. BRTs are an ensemble-approach, in which a prediction \hat{y}_i is based on the weighted sum of the predictions of progressively “less important” regression trees (t_k), as opposed to the predictions of one tree (Elith et al., 2008). For $k \rightarrow nt$ number of trees, where each tree is itself a function of the matrix \mathbf{X} of j predictor variables ($t_k = f(x_{ij})$), a BRT-model can be represented as follows:

$$\hat{y}_i = \sum_{k=1}^{nt} w_k t_k \quad (3)$$

BRTs have two major meta-parameters over which users have control (???): the learning rate (lr , the rate at which iterative trees reduce predictive deviance during model-training, controlling the contribution of each tree

230 to the final model) and tree complexity (tc , the number of nodes on a given regression-tree, i.e. the maximum
231 interaction depth the model is permitted to fit).

232 BRTs were implemented here to predict both vascular plant species richness and turnover in each HDS, as a
233 function of environmental variables and environmental roughness values in those cells, as Gaussian responses,
234 thus resulting in two BRT-models for each region. We treated richness as S_{HDS} and turnover as \bar{J}_{QDS} . The
235 natural logarithm of species richness was used, in order to satisfy the assumptions of a Gaussian response.
236 Note, this is not strictly because BRTs have any parametric assumptions concerning the distribution of the
237 response variable, but rather to aid in applying the Gaussian-family of BRT algorithms to the richness data
238 available. Additionally, BRTs were implemented to predict vascular plant species richness at the QDS-scale
239 (S_{QDS}), thus resulting in a total of six BRT-models presented here.

240 As recommended by Elith et al. (2008), BRT models were trained on a set of non-collinear predictor variables
241 using “gbm.step” in “dismo” (???) and “gbm” (???). Collinear predictor variables can skew the interpretation
242 of results, as the relative influence of mutually collinear variables is reduced. Collinearity among the nine
243 environmental predictor variables and their respective nine roughness-equivalents was assessed using
244 “removeCollinearity” in the R package “virtualspecies” (???) separately for each region, such that variables
245 were no more than 80% collinear (Pearson’s $r \geq 0.80$). When faced with a cluster of collinear variables, one
246 variable was chosen manually therefrom. Where possible, the roughness-equivalent of an environmental
247 variable was included if its absolute-equivalent could also be included. When interpreting the results of BRTs,
248 it is important to consider the effects of the variables included as representative of the effect of the excluded
249 variables with which it was found to be collinear.

250 In order to select ideal lr and tc all models (described below) were trained on the final non-collinear predictor
251 sets iteratively for 25 combinations of a range of tc values (1 to 5) and a range of lr values (0.01, 0.005, 0.001,
252 5×10^{-4} , 1×10^{-4}). The function “gbm.step” optimises the number of trees (nt) using cross-validation during
253 model training (Elith et al., 2008) by halting iteration when predictions begin to overfit. For all models, we
254 used 10 cross-validation folds (i.e. use 10 different randomly selected training data sets), a tolerance-threshold
255 of 0.001, a bagging-fraction of 0.75 (proportion of training data randomly chosen to generate each tree), and
256 trained models starting with 50 trees, with each iterative step adding 50 trees at a time, up to a maximum of
257 10,000 trees. Following this iterative parameter optimisation, Gaussian BRT models were constructed with
258 $tc = 3$ and $lr = 0.001$, along with the other settings described.

259 The optimum configuration of lr and tc for the final model is a trade-off between model fit (e.g. pseudo- R^2 ;

Equation (4)) and complexity (nt). A tc of 5 was chosen for the final model. This follows the recommendations of Elith et al. (2008), where lr and tc are advised to be adjusted inversely. This was chosen in order to account for the complex interactions determining species richness. To avoid overfitting, an intermediate lr of 0.001 was chosen.

2.4.4 Assessing BRT-predictions' fit

BRT-model performance can be described by measuring the variance in a dataset a BRT-model has explained, quantified here by R^2_{pseudo} , which is the proportion of null deviance D_{null} explained by some model i . Formally, it is defined as follows:

$$R^2_{\text{pseudo}} = 1 - \frac{D_i}{D_{\text{null}}} \quad (4)$$

The derivation of this metric is not easy to interpret, as it is not immediately clear what model deviance is. Alternatively, comparing expected (i.e. model-predicted) and observed data has more heuristic appeal. We employed this metric of BRT-model performance too. We regressed expected against observed richness and turnover, and calculated the R^2 -value for those regressions (hereafter $R^2_{\text{E-O}}$).

The BRT-model fitting algorithm contains intrinsic stochasticity, due to the random partitions made in a dataset during cross-validation. Though this randomness is usually negligible (e.g. variables' contributions vary from run-to-run by a few decimal places), we reran each of the six BRT-models (see above) 1000 times in order to account for this stochasticity. Where indicated, we either present the averages of these replicate-models' results or the results of a representative model from each set of replicates.

In order to assess the reliability of the conclusions drawn from these models, we randomly permuted the response data (S_{QDS} , S_{HDS} and \bar{J}_{QDS}) with respect to the environmental and heterogeneity data, and reran all six BRT-models 999 times (with the final non-collinear predictor sets and preconfigurations above). This also allows us to remove any effect of spatial autocorrelation in generating the observed correlations between patterns of species occurrence and environment (???), and to allow us to assess the significance of our results relative to a random null. Notably, as the predictor variables themselves are likely spatially autocorrelated, correlation structure in model residuals is accounted for by the correlation structure in the environmental data. Nonetheless, we wished to demonstrate our results more robustly and thus carried out these permutation tests. For all six models, the majority of the 999 permuted models failed to find associations between the response

and predictor variables. The results of those that succeeded to fit a model to completion (usually ca. 200 out of 999) are presented. The replicate and permuted BRT-models were compared using various measures of model performance (above; nt , R_{pseudo}^2 (Equation (4)), $R_{\text{E-O}}^2$) and the ranks of these values for each replicate BRT-model relative to the 999 permuted models for that region/scope.

3 Results

3.1 Describing environmental heterogeneity across scales

Across all variables considered, the Cape is more environmentally heterogeneous in the majority of pairwise comparisons of grid-cells ($CLES > 0.50$, Mann-Whitney U -test: $P < 0.05$, Figure 1). The Cape is thus more environmentally heterogeneous than SWA overall, but the degree to which it is more heterogeneous varies between environmental variables. These effects also vary somewhat with the spatial scale concerned. In some variables, the differentiation between Cape and SWA heterogeneity lessens at coarser scales (Figure 1b). Indeed, when comparing the overall ranking and medians of Cape vs SWA roughness values for each variable, we only find non-significant differences at the coarser 3QDS scale (Mann-Whitney U tests, $P > 0.05$, Figure 1b).

Most obviously, and as expected, topographic heterogeneity is greatest in the Cape (Figure 1). Though SWA has a slightly wider distribution of elevational roughness values at coarse scales (e.g. 3QDS) compared to fine scales (0.05°), so does the Cape. As such, the relative difference in heterogeneity between the two regions seems invariant with spatial scale ($CLES \approx 0.95$, Figure 1b). This concurs with our expectations, as the Cape is mountainous and known to have steep elevational gradients (??), while SWA is much more topographically uniform. Intuitively, then, elevation serves as a “benchmark test” for our comparisons of EH here, as it is well known and expected that the Cape should be more elevationally heterogeneous than SWA.

Climatic heterogeneity is less differentiated between the Cape and SWA than elevational roughness (Figure 1a), though still the Cape is indeed more climatically heterogeneous (Figure ??b). Notably, the difference between Cape and SWA mean annual rainfall and land surface temperature heterogeneities is less pronounced when considered at coarse spatial scales (3QDS scale, Figure ??b). Rainfall seasonality (PDQ), however, is similarly more heterogeneous in the Cape across all spatial scales considered.

Biological productivity, as measured by NDVI, varies spatially to a similar extent in the Cape and SWA (i.e. is

313 more similarly heterogeneous, $CLES < 0.60$, Figure 1).

314 Concerning edaphic variables, the Cape and SWA are similarly heterogeneous at coarser scales, particularly in
315 terms of CEC and Soil C ($CLES \approx 0.50$, Figure 1b).

316 **3.2 Comparing species turnover in the two regions**

317 Following calculations of \bar{J}_{QDS} and T_{HDS} for each HDS-cell in each region, we used non-parametric
318 Mann-Whitney U -tests to compare the distributions of values in the Cape and SWA. The Cape possesses
319 generally greater floristic turnover than SWA, for both measures of turnover defined here ($P < 0.0001$, Figure
320 2a,b). Being derived from Jaccard distances, \bar{J}_{QDS} measures the average pairwise proportional floristic
321 turnover between QDS in each HDS. T_{HDS} , however, represents the β component of γ -diversity. As
322 γ -diversity (S_{HDS}) in the Cape is more greatly a function of β -diversity (T_{HDS}) than in SWA, the
323 complement is necessarily true: γ -diversity in the Cape is less a function of α -diversity (\bar{S}_{QDS}) than in SWA.

324 **3.3 Predicting richness and turnover with environmental heterogeneity**

325 Vascular plant species richness and turnover are found to both be predicted primarily by environmental
326 heterogeneity in the Cape (Figure 3a–c) and at least in-part by environmental heterogeneity in SWA (Figure
327 3d–f). Our six BRT-models performed adequately, and detected relationships between patterns of species
328 occurrence and the environment that do not occur in the permuted datasets (Figures 4 and 3, Table 2).

329 BRT-models of species richness at the QDS-scale in each region seemed to generally performed best, as these
330 models had generally fit the greatest number of trees (nt , Figure 4a), and higher R^2 -values (Figure 4b,c).
331 Notably, SWA models of species richness and turnover at the HDS-scale out-performed Cape models, while at
332 the QDS-scale the Cape models performed as-well or better (Figure 4, Table 3).

333 Across our BRT-models of species richness and turnover, the sets of environmental variables important to
334 model predictions differ substantially between the Cape and SWA, both in terms of which aspects of the
335 environment were found to be biologically relevant and in terms of the relative importance of absolute and
336 heterogeneity variables (Figure 3). Most obviously, species richness and turnover in the Cape are predicted in
337 majority by environmental heterogeneity, which is not the case in SWA (piecharts inset Figure 3). Species
338 richness and turnover in the Cape are predicted by a broad suite of environmental variables, with no individual

variable contributing more than ca. 20% to any model prediction (Figure 3a–c). The SWA models' predictions, however, are largely determined by MAP (Figure 3d–f).

Species richness at QDS-scales, and to a lesser extent at HDS-scales, in the Cape is predicted in large part by edaphic conditions (Figure 3a,b). Contrastingly, richness in SWA across both scales is mostly predicted by MAP and other climatic variables (Figure 3d,e). Interestingly, topographic heterogeneity did not feature as highly in contributing to Cape predictions as we expected (Figure 3a–c).

It is important to consider variables not included formally in these BRT-models that were found to be collinear with some of the variables included (see SI). Here, we interpret the effects of variables excluded from the analyses as well as those included, as the forms and importances of these relationships are likely similar.

In the Cape (concerning clusters of collinear variables relevant to those retained during BRT-model fitting), MAP was included in the BRT-analyses as representative of a cluster of collinear variables consisting of itself, NDVI, surface T and soil C at the. Roughness in soil clay content represented itself, roughness in soil pH and roughness in NDVI. In SWA, MAP was selected as representative of itself, NDVI and soil C.

In the equations below, collinear groups of variables are listed as predictors enclosed within braces.

Cape:

$$\begin{aligned}
 \bar{S}_{QDS} &\sim pH + R_{SurfT} + \left\{ \begin{array}{c} MAP \\ NDVI \\ SurfT \\ SoilC \end{array} \right\} + \left\{ \begin{array}{c} R_{Clay} \\ R_{pH} \end{array} \right\} + RElev \\
 S_{HDS} &\sim R_{SurfT} + RElev + R_{CEC} + \left\{ \begin{array}{c} R_{MAP} \\ R_{PDQ} \\ R_{NDVI} \end{array} \right\} + \left\{ \begin{array}{c} MAP \\ NDVI \\ SurfT \\ SoilC \end{array} \right\} \\
 T_{HDS} &\sim RElev + R_{SurfT} + \left\{ \begin{array}{c} R_{MAP} \\ R_{PDQ} \\ R_{NDVI} \end{array} \right\} + Elev + R_{CEC}
 \end{aligned}$$

SWA:

$$\begin{aligned}\bar{S}_{QDS} &\sim \begin{Bmatrix} MAP \\ NDVI \\ SoilC \end{Bmatrix} + PDQ + RMAP \\ S_{HDS} &\sim \begin{Bmatrix} MAP \\ NDVI \\ SoilC \end{Bmatrix} + CEC + RElev \\ T_{HDS} &\sim \begin{Bmatrix} MAP \\ NDVI \\ SoilC \end{Bmatrix} + RElev + CEC\end{aligned}$$

Our BRT-models of species richness at QDS- and HDS-scales, in both regions, rank environmental variables somewhat differently (Figure 3a,b,d,e), though these differences are slightly less extreme than would be expected by chance ($P_{1-2} < 0.01$, Figure 5). This suggests a weak, but measurable, scale-dependence of the importance of different environmental variables' associations with species richness.

It is noteworthy that BRT-models of species turnover (at HDS-scales) (Figure 3c,f) rank variables similarly to models of richness at HDS-scales ($P_{2-3} \leq 0.005$, Figure 5). This is likely due to the fact that species turnover covaries with species richness. As such, though the signs of relationships determining turnover may differ from those determining richness, the importances of different variables would be similar.

In addition to different variables being more strongly associated with species richness and turnover in the Cape compared to SWA (Figure 3), the forms of those relationships vary (Figure 6). We found MAP, and roughness therein, to relate positively with species richness in both regions at both scales (Figure 6a,b,d,e). As MAP is collinear with NDVI and soil C in both regions (and surface T in the Cape), this can be interpreted as the signal of a biological productivity and resource availability associating with high levels of species richness.

The positive association of heterogeneity variables in the Cape as opposed to SWA (Figure 6a,b vs d,e) concurs with their greater importance in BRT-model predictions (Figure 3).

The fact that species turnover ($T_{HDS} = \bar{J}_{QDS}$) in the Cape and SWA is largely predicted by the same variables as species richness, but with opposite signs to its relationships (Figure 6c,f), is indicative of the richness-dependence of the measure of floristic turnover used here (Jaccard distances) to quantify turnover at the HDS-scale.

4 Discussion

I have provided support for the hypothesis that the difference in plant species richness between the GCFR and SWAFR is accounted for by the fact that the GCFR is more abiotically heterogeneous than the SWAFR. As expected, the GCFR is shown to possess (i) a quantifiably more heterogeneous environment, and (ii) is heterogeneous at a finer spatial scale than the SWAFR. I have shown that vascular plant species richness (iii) can be explained in terms of environmental conditions, including environmental heterogeneity, in both the GCFR and SWAFR. Also, I have shown that (iv) the set of environmental axes that explain plant species richness, both absolute and as heterogeneity, differs between the GCFR and SWAFR. These findings contribute towards an understanding of the ecological conditions that facilitate species coexistence (and likely stimulate ecological speciation) in these two regions.

These two regions present differentiable environmental spaces, each with heterogeneity varying across spatial scales. The clear separation of the regions' topographic features is as expected (Figures ??A, ??). Indeed, topography seems to be the most striking distinction between the regions. The Cape region has been found previously to have the second highest median topographic heterogeneity of the five Mediterranean-climate regions (Bradshaw & Cowling, 2014). The GCFR has a much wider range of scales exhibited in the heterogeneity across its environmental axes. Notably, each region has finer scale heterogeneity in some variables, and coarser scale in others—neither region is necessarily more fine or coarse than the other, as it depends on the variable concerned. BRT-models of species richness in both regions reveal species richness to depend on those environmental axes that differentiate the two regions (Figures ??, ??). The importance of variables is also shown to vary with spatial scale (Figure ??), as previously suggested may be the case when modelling geographic patterns of biodiversity (Baudena et al., 2015). Indeed, as Cowling et al. (1996) describes differing patterns of species richness across spatial scales, so do the predictors of those patterns vary with scale (Hart et al., 2017).

The fact that a combination of absolute and roughness variables is also as predicted by the hypothesis in this study. In the models developed by Cramer & Verboom (2016) for South Africa, roughness in topography was largely superseded as an important predictor of species richness by other roughness variables. My models, however, did not show this. Similar to the study by Rensburg et al. (2002), my models revealed roughness in topography and other variables to be important. Although, Rensburg et al. (2002) considered differences within pixels, as opposed to this study, which considered differences between pixels. My models, those of Cramer & Verboom (2016), and those of Rensburg et al. (2002), do not all concur as to the role of roughness in

elevation vs. more biologically meaningful variables in explaining species richness. The source of these discrepancies is unclear, though no doubt complex. The complements of environmental variables and methodologies used in these studies do differ, limiting extensive comparison between these analyses.

The determinants of vascular plant species are shown to be region specific (Figures ??, ??, ??). The importance of MAP and roughness in rainfall seasonality (PCV) in predicting richness in the SWAFR (Figure ??I, ??J), aligns with the steep climatic gradients observed there (Cook et al., 2015). The soil variables that determine plant species richness in the model for the SWAFR (Figures ??K, ??L) differ to those that determine richness in the GCFR (Figures ??G, ??H), further highlighting the edaphic differences between these two regions.

Although both are nutrient leached systems, the SWAFR is flat, with soil-chronosequences (Laliberte et al., 2014; Cook et al., 2015), while the GCFR is mountainous (Cowling et al., 1996; Cramer et al., 2014; Verboom et al., 2017). The importance of roughness in soil density, and absolute texture, in the SWAFR (Figures ??K, ??L) highlights the changes in soil that are associable with age of the substrate (e.g. particle size) as being biologically relevant to species richness. The positive effect of soil clay content on species richness in the SWAFR aligns with the findings of Laliberte et al. (2014) that richness in the SWAFR increases with soil age.

NDVI is more heterogeneous across the GCFR than the SWAFR (Figures ??A). The fact that thermal variables tend to be more rough in the GCFR (Figure ??A) is likely due to possible covariance of the MODIS/Terra products with topography, as MODIS data used here describes land surface temperature. As the GCFR is topographically rugged, the roughness of NDVI may arise from this. Despite this, NDVI is an integrating variable, which captures information about productivity, light availability, and soil nutrients (Power et al., 2017). The fact that absolute NDVI contributes to predicting species richness in the GCFR, especially at finer spatial scales (Figure ??E) demonstrates the role of ecological productivity in facilitating the coexistence diverse species assemblages. Environmental heterogeneity, then, is integral to explaining patterns of species richness, but must be considered along with resource- and energy-availability axes. In so much as a diverse environmental space supports more species, the materials and productivity required for biota to thrive are also needed to support species (???; Gaston, 2000; Bohn & Amundsen, 2004; Kreft & Jetz, 2007). As such, my findings, along with those of previous studies (Rensburg et al., 2002; Thuiller et al., 2006; Kreft & Jetz, 2007; Cramer & Verboom, 2016), suggest that there is ecological and evolutionary consequence to resource availability *and* environmental heterogeneity, in that they tend to be positively associated with species richness.

The combined BRT-model of species richness for both regions reveals soil clay content as an important predictor, at coarse spatial scales, despite this variable not being particularly important within each region

434 separately (Figure ??). Though this model does not strictly consider the regions as separate, this finding may
435 indicate that the relationship between clay content and species richness differs between the regions. So far as
436 clay content can be used to predict species richness, it matters more to those predictions when applied to large
437 sections (i.e. coarse scales) of each regions.

438 Kreft & Jetz (2007) modelled global terrestrial vascular plant species richness, which focussed on primarily
439 absolute environmental values, underestimated the richness of the Cape flora. Though Kreft & Jetz (2007) did
440 include topographic heterogeneity in their predictor set, topography is often a proxy for more biologically
441 meaningful variables (Cramer & Verboom, 2016). This explains why the inclusion of these variables
442 (e.g. roughness in mean annual precipitation) yields more accurate predictions of species richness. Indeed,
443 Thuiller et al. (2006) also included topographic heterogeneity. Cramer & Verboom (2016) described 68% of
444 species richness at the QDS scale across South Africa. Regarding the GCFR, depending on whether one
445 consults pseudo- R^2 (Table 3), the ratio of mean predicted to observed richness per grid-cell (Table 5), or the
446 distributions of predicted vs. observed richness values per grid-cell (Figure ??), I have achieved a similarly
447 suitable level of predictive accuracy. There is, though, still unexplained species richness in light of my models.
448 As Cramer & Verboom (2016), Rensburg et al. (2002), Thuiller et al. (2006), and Mouchet et al. (2015) have
449 done, these macro-ecological models are a-historical. Evolutionary considerations of species richness in
450 geographic space are worthwhile, especially in regions with environments stable over evolutionary time.

451 The findings here are correlative. There are, however, many proposed mechanisms to explain the correlative
452 signals demonstrated here. My findings support the hypothesis that Mediterranean systems' plant species
453 richness is a function of spatial variability in environmental conditions. This can stimulate diversification, and
454 maintain that diversity by providing a range of habitats for species co-existence. Oligotrophic soils can stimulate
455 an increase in functional diversity, through the evolution of diverse nutrient acquisition strategies (Lambers et
456 al., 2010; Verboom et al., 2017)—e.g. sclerophylly (Cramer et al., 2014; Cook et al., 2015). An aspect of the
457 environment I have neglected to consider is fire, shown to also contribute to predictions here in the GCFR
458 (Cramer & Verboom, 2016). Cardillo (2012) have shown the structuring forces behind species co-occurrence
459 patterns, and thus likely species richness, differ between species-pairs with different post-fire responses and
460 those with similar post-fire responses.

461 Though the GCFR was correctly predicted to have, on average, more species per grid-cell at HDS and 3QDS
462 scales than the SWAFR, this was not the case for QDS grid-cells (Table 5). This demonstrates that the GCFR is
463 indeed overall more rich in plant species than the SWAFR, but a given HDS in the SWAFR contains fewer

species than a given GCFR HDS. Thus, the greater richness in the GCFR is a product of greater turnover in species at spatial scales no more coarse than the HDS. Species turnover is an interesting aspect to species richness studies, as it species turnover is implicit to species-area and co-existence-area relationships (Hart et al., 2017). One could expect patterns of endemism and species turnover to concur with patterns in environmental heterogeneity to some degree.

Following from the understanding that functionally diverse assemblages, which are more likely to be more species rich, are likely to arise and/or occur in areas with diverse ecological pressures (Molina-Venegas et al., 2015), one would expect, then, heterogeneous habitats such as those in Mediterranean-type biodiversity hotspots to exhibit high levels functional beta diversity along steep environmental gradients (Molina-Venegas et al., 2015). If the niches concerning these functions are phylogenetically conserved among those biota, then one would also expect high levels of species and phylogenetic beta diversity along these gradients (Molina-Venegas et al., 2015). This concurs with the notion put forward by Power et al. (2017), wherein megadiverse systems such as these represent the results of “phylogenetic niche conservatism on a heterogeneous landscape”. Thus, species and phylogenetic turnover should covary with environmental heterogeneity in some way. Indeed, endemism, at certain scales, could also follow this pattern. Thuiller et al. (2006) demonstrated that there is phylogenetic and biome related determinants of species richness. This makes sense, in light of the difficulty of crossing biome boundaries in Mediterranean systems (Power et al., 2017). NDVI and light availability, and the heterogeneity therein, are associated with high levels of floristic turnover (Power et al., 2017). This may be indicative of ecological specialisation precluding species from crossing these boundaries, thus increasing the level of endemism within a region, while also increasing the level of turnover, and thus likely species richness, along environmental gradients. Although, this may be debated. Beard et al. (2000) state that the high levels of endemism in SWAFR are function of habitat specialisation to soil mosaics. Cf. Laliberte et al. (2014), who say that this endemism is likely due to environmental filtering along these soil turnover sequences, as opposed to the juxtaposition of specialised species along soil gradients.

I have demonstrated support for the idea that environmental heterogeneity is positively associated with species richness, particularly Mediterranean systems. In the SWAFR and the GCFR, high levels of endemism and biodiversity are also likely the results of long-term landscape and climatic stability (Hopper, 1979). Thus, the roles of environmental variability through space, and stability through time, are the two main ways in which the environment relates to biodiversity in these regions.

4.1 Future studies (a.k.a. “to do after first review”)

- 3QDS scale BRTs
- $S_{\text{HDS}} \sim \bar{S}_{\text{QDS}} + \bar{\delta}_{ij}??$ (= “ $\gamma = \alpha + \beta$ ”-analysis) (see `explore-turnover-metrics.pdf` note, where $\bar{\delta}_{ij}(\mathbf{N})?? = \bar{\alpha}_i(\mathbf{N}) \times \bar{\beta}_{ij}(\mathbf{N}) = \bar{S}_{\text{QDS}} \times \bar{J}_{\text{QDS}}$)

Table captions

Captions are also repeated alongside their respective tables for readability.

Table 1: Georeferenced vascular plant species occurrence and environmental data sources used in this study. Data were acquired for the Cape and SWA regions, with the temporal extent of data products used described where applicable. Abbreviations are as follows: MAP, mean annual precipitation; PDQ, precipitation in the driest quarter; CEC, cation exchange capacity.

Table 2: Average percentile-ranks for BRT-model performance measures (nt , R_{pseudo}^2 (Equation (4)), $R_{\text{E-O}}^2$) of 1000 replicate BRT-models relative to 999 BRT-models fit to permuted datasets. Ranks approaching one indicate that a set of replicate BRT-models had greater values than the permuted models.

Table 3: Estimated differences between replicate Cape and SWA BRT-models’ performance measures (nt , R_{pseudo}^2 (Equation (4)), $R_{\text{E-O}}^2$) following t -tests. Positive values indicate that the Cape models had greater values. In all cases, the Cape and SWA had highly significantly different values for these quality measures ($P < 0.0001$).

Figure captions

Captions are also repeated alongside their respective figures for readability.

Figure 1: Types of environmental heterogeneity, compared between the the Cape and SWA—namely for (a) elevation, (b) climatic variables, (c) NDVI and (d) soil variables—in each panel consisting of three sub-panels per variable type. The upper row of panels shows example distributions of roughness values (Equation (1)), showing the different extremes in environmental heterogeneity observed in each region when compared at fine (0.05°) and coarse (3QDS) scales. Each distribution has under it an area of one. Histograms were constructed

517 using 20 breaks. In the lower row of panels, these distributions of roughness values were compared between
 518 the Cape and SWA at each of the four spatial scales, not just 0.05° and 3QDS, using non-parametric
 519 Mann-Whitney U -tests to test for differences. The “common language effect size” ($CLES$, see text) describes
 520 these differences (b). U -tests for almost all environmental variables yielded significant differences ($P < 0.05$)
 521 between Cape and SWA values (NS, non-significant differences). $CLES$ for 0.05 res. is for 5000 random cells
 522 in each region, as the Mann-Whitney U -test cannot handle more than a few thousand values per sample when
 523 comparing.

524 Figure 2: Species turnover, described in two forms ((a) mean Jaccard distance between QDS in each HDS
 525 (\bar{J}_{QDS}), (b) additively defined turnover (T_{HDS} , Equation (2)) as a proportion of HDS richness (S_{HDS})),
 526 compared between the Cape and SWA. Mann-Whitney U -tests between the Cape and SWA distributions of
 527 \bar{J}_{QDS} and T_{HDS} yielded significant differences.

528 Figure 3: Relative influence of environmental variables (including heterogeneity variables—prefixed with “R”)
 529 in boosted regression tree (BRT) model predictions for the final six models’ response variables in the Greater
 530 Cape Floristic Region (Cape) and the Southwest Australia Floristic Region (SWA): vascular plant species
 531 richness at the (b,e) QDS-scale, (a,d) HDS-scale and (c,f) turnover ($= \bar{J}_{QDS}$). All BRT-models were permitted
 532 to fit three-way interactions between environmental variables. Points denote the average contribution of an
 533 environmental variable to model-predictions across the 1000 replicate BRT-models for that region/scope.
 534 Horizontal ticks denote the average for the 999 permuted BRT-models. The standard deviations above and
 535 below these means are shown with vertical lines. Note that in the case of the replicate models they are very
 536 small in most cases, obscuring them. Colour represents the general category of the environment (keyed) to
 537 which a variable belongs, as in Figure 1b. Piecharts inset display the same information (left-most piecharts),
 538 and additionally grouped according to whether a variable was absolute or roughness-transformed (right-most
 539 piecharts). F -statistics inset are for one-way ANOVAs of differences in variables’ relative influences from the
 540 replicate ($F_{rep.}$) and permuted ($F_{prm.}$) BRT-models.

541 Figure 6: Marginal effects of environmental conditions and heterogeneity on vascular plant species richness at
 542 the QDS-scale (a, d), HDS-scale (b, e) and turnover ($= \bar{J}_{QDS}$; c, f) in response variables in the Greater Cape
 543 Floristic Region (Cape; a–c) and Southwest Australia Floristic Region (SWA; d–f) following boosted
 544 regression tree (BRT) modelling. Marginal effect functions presented are derived from a representative
 545 BRT-model from the set of replicate BRT-models (for each of the six modelling cases) (see SI regarding how
 546 representative BRT-models were selected). Marginal effect functions are shown for environmental variables

that contributed $\geq 10\%$ to a model's predictions. Functions are coloured as keyed, with solid lines representing absolute environmental variables and dotted representing heterogeneity variables ("rough"). Environmental variables were all rescaled here such as to be centred on zero facilitating comparison of functions' forms.

Figure 4: Distributions of three measures of boosted regression tree (BRT) model performance (a) the number of trees in the model nt , (b) R^2_{pseudo} (Equation (4)), (c) $R^2_{\text{E-O}}$ (see text). These measures are presented for the six sets of permuted (pale bars) and six sets of replicate BRT-models (dark bars) as in Figure 3, coloured according to the region of interest as in Figures 1a and 2. In all cases, replicate BRT-models almost entirely out-rank the permuted models in terms of performance (Table 2) and Cape and SWA models had significantly different values for each metric (Table 3). Note, the actual differences between Cape and SWA models' values is not realistically important in some cases.

Figure 5: Differences in the rankings of environmental variables' (including heterogeneity variables) relative influences on boosted regression tree (BRT) model predictions of vascular plant species richness and turnover in (a) Cape and (b) SWA (as in Figure 3). Each point represents an environmental variable's rank in BRT-model importance, decreasing in importance from left to right. Rankings used here are the same as that of the average relative influence for variables across replicate BRT-models, presented in Figure 3. Coloured lines connect points representing the same environmental variable. Points' outlines are coloured according to the general category of the environment (keyed) to which a variable belongs, as in Figure 1b and 3, while points' centres are coloured according to whether a variable was roughness-transformed or not. The comparisons of variables' rankings of interest are between QDS- and HDS-scale richness (rows nos. 1 and 2) and between HDS-scale richness and turnover (rows nos. 2 and 3). Statistics (Δ - and P -values) inset at the top and bottom of each panel refer to these comparisons respectively. Δ -values represent the average absolute difference in ranks across variables between two models' rankings. The associate P -value results from ranking the observed Δ -values against 999 Δ -values based on random permutations of variables' rankings (SI1), such that more significant P -values denote rankings more similar than would be expected by chance.

References

- Baudena, M., Sánchez, A., Georg, C.-P., Ruiz-Benito, P., Rodríguez, M.Á., Zavala, M.A., & Rietkerk, M. (2015) Revealing patterns of local species richness along environmental gradients with a novel network tool. *Scientific Reports*, **5**, 11561.
- Beard, J.S., Chapman, A.R., & Gioia, P. (2000) Species richness and endemism in the Western Australian flora. *Journal of*

- 575 *Biogeography*, **27**, 1257–1268.
- 576 Bøhn, T. & Amundsen, P.-A. (2004) Ecological Interactions and Evolution: Forgotten Parts of Biodiversity? *BioScience*, **54**, 804.
- 577 Bradshaw, P.L. & Cowling, R.M. (2014) Landscapes, rock types, and climate of the Greater Cape Floristic Region. *Fynbos: Ecology,*
578 *evolution and conservation of a megadiverse region* (ed. by N. Allsopp, J.F. Colville, and G.A. Verboom), pp. 26–46. Oxford
579 University Press, Oxford.
- 580 Cardillo, M. (2012) The phylogenetic signal of species co-occurrence in high-diversity shrublands: different patterns for fire-killed and
581 fire-resistant species. *BMC Ecology*, **12**, 21.
- 582 Cook, L.G., Hardy, N.B., & Crisp, M.D. (2015) Three explanations for biodiversity hotspots: small range size, geographical overlap
583 and time for species accumulation. An Australian case study. *New Phytologist*, **207**, 390–400.
- 584 Cowling, R.M., Rundel, P.W., Lamont, B.B., Arroyo, M.K., & Arianoutsou, M. (1996) Plant diversity in mediterranean-climate
585 regions. *Trends in Ecology and Evolution*, **11**, 362–366.
- 586 Cramer, M.D. & Verboom, G.A. (2016) Measures of biologically relevant environmental heterogeneity improve prediction of regional
587 plant species richness. *Journal of Biogeography*, 1–13.
- 588 Cramer, M.D., West, A.G., Power, S.C., Skelton, R., & Stock, W.D. (2014) Plant ecophysiological diversity. *Fynbos: Ecology,*
589 *evolution and conservation of a megadiverse region* pp. 248–272. Oxford University Press, Oxford.
- 590 Deblauwe, V., Droissart, V., Bose, R., Sonké, B., Blach-Overgaard, A., Svenning, J.C., Wieringa, J.J., Ramesh, B.R., Stévant, T., &
591 Couvreur, T.L.P. (2016) Remotely sensed temperature and precipitation data improve species distribution modelling in the
592 tropics. *Global Ecology and Biogeography*, **25**, 443–454.
- 593 Elith, J., Leathwick, J.R., & Hastie, T. (2008) A working guide to boosted regression trees. *Journal of Animal Ecology*, **77**, 802–813.
- 594 Farr, T., Rosen, P., Caro, E., Crippen, R., Duren, R., Hensley, S., Kobrick, M., Paller, M., Rodriguez, E., Roth, L., Seal, D., Shaffer, S.,
595 Shimada, J., Umland, J., Werner, M., Oskin, M., Burbank, D., & Alsdorf, D. (2007) The shuttle radar topography mission.
596 *Reviews of Geophysics*, **45**, 1–33.
- 597 Funk, C.C., Peterson, P.J., Landsfeld, M., Pedreros, D.H., Verdin, J., Shukla, S., Husak, G., Rowland, J.D., Harrison, L., Hoell, A., &
598 Michaelsen, J. (2015) The climate hazards infrared precipitation with stations—a new environmental record for monitoring
599 extremes. *Scientific Data*, **2**, 150066.
- 600 Gaston, K.J. (2000) Global patterns in biodiversity. *Nature*, **405**, 220–227.
- 601 GBIF (24 July 2017) GBIF Occurrence Download..
- 602 GBIF (24 July 2017) GBIF Occurrence Download..
- 603 Gioia, P. & Hopper, S.D. (2017) A new phytogeographic map for the Southwest Australian Floristic Region after an exceptional decade

604 of collection and discovery. *Botanical Journal of the Linnean Society*, **184**, 1–15.

605 Hart, S.P., Usinowicz, J., & Levine, J.M. (2017) The spatial scales of species coexistence. *Nature Ecology & Evolution*, **1**, 1066–1073.

606 Hengl, T., Mendes de Jesus, J., Heuvelink, G.B.M., Ruiperez Gonzalez, M., Kilibarda, M., Blagoti?, A., Shangguan, W., Wright, M.N.,
607 Geng, X., Bauer-Marschallinger, B., Guevara, M.A., Vargas, R., MacMillan, R.A., Batjes, N.H., Leenaars, J.G.B., Ribeiro, E.,
608 Wheeler, I., Mantel, S., & Kempen, B. (2017) SoilGrids250m: Global gridded soil information based on machine learning.
609 *PLoS ONE*, **12**, e0169748.

610 Hopper, S.D. (1979) Biogeographical Aspects of Speciation in the Southwest Australian Flora. *Annual Review of Ecology and*
611 *Systematics*, **10**, 399–422.

612 Hopper, S.D. & Gioia, P. (2004) The Southwest Australian Floristic Region: Evolution and Conservation of a Global Hot Spot of
613 Biodiversity. *Annual Review of Ecology, Evolution, and Systematics*, **35**, 623–650.

614 Kreft, H. & Jetz, W. (2007) Global patterns and determinants of vascular plant diversity. *Proceedings of the National Academy of*
615 *Sciences*, **104**, 5925–5930.

616 Laliberte, E., Zemunik, G., & Turner, B.L. (2014) Environmental filtering explains variation in plant diversity along resource gradients.
617 *Science*, **345**, 1602–1605.

618 Lambers, H., Brundrett, M.C., Raven, J.A., & Hopper, S.D. (2010) Plant mineral nutrition in ancient landscapes: high plant species
619 diversity on infertile soils is linked to functional diversity for nutritional strategies. *Plant and Soil*, **334**, 11–31.

620 Larsen, R., Holmern, T., Prager, S.D., Maliti, H., & Røskaft, E. (2009) Using the extended quarter degree grid cell system to unify
621 mapping and sharing of biodiversity data. *African Journal of Ecology*, **47**, 382–392.

622 Levin, L.A., Sibuet, M., Gooday, A.J., Smith, C.R., & Vanreusel, A. (2010) The roles of habitat heterogeneity in generating and
623 maintaining biodiversity on continental margins: an introduction. *Marine Ecology*, **31**, 1–5.

624 Lobo, J.M., Jay-robert, P., Lumaret, J.-p., Lobo, J.M., Jay-robert, P., & Lumaret, J.-p. (2004) Modelling the Species Richness
625 Distribution for French Aphodiidae (Coleoptera, Scarabaeoidea). *Ecography*, **27**, 145–156.

626 Mateo, R.G., Mokany, K., & Guisan, A. (2017) Biodiversity Models: What If Unsaturation Is the Rule? *Trends in Ecology &*
627 *Evolution*, **32**, 556–566.

628 Molina-Venegas, R., Aparicio, A., Slingsby, J.A., Lavergne, S., & Arroyo, J. (2015) Investigating the evolutionary assembly of a
629 Mediterranean biodiversity hotspot: Deep phylogenetic signal in the distribution of eudicots across elevational belts. *Journal*
630 *of Biogeography*, **42**, 507–518.

631 Mouchet, M., Levers, C., Zupan, L., Kuemmerle, T., Plutzar, C., Erb, K., Lavorel, S., Thuiller, W., & Haberl, H. (2015) Testing the
632 effectiveness of environmental variables to explain European terrestrial vertebrate species richness across biogeographical

scales. *PLoS ONE*, **10**, 1–16.

Mucina, L. & Rutherford, M.C. (2006) *The vegetation of South Africa, Lesotho and Swaziland*. South African National Biodiversity Institute,

NIMA (2000) Amendment 1. 3 January 2000. Department of Defense World Geodetic System 1984. Its Definition and Relationships with Local Geodetic Systems. 1–3.

Olson, D.M., Dinerstein, E., Wikramanayake, E.D., Burgess, N.D., Powell, G.V.N., Underwood, E.C., D’amico, J.A., Itoua, I., Strand, H.E., Morrison, J.C., & Others (2001) Terrestrial Ecoregions of the World: A New Map of Life on Earth: A new global map of terrestrial ecoregions provides an innovative tool for conserving biodiversity. *BioScience*, **51**, 933–938.

Power, S.C., Verboom, G.A., Bond, W.J., & Cramer, M.D. (2017) Environmental correlates of biome-level floristic turnover in South Africa. *Journal of Biogeography*, **44**, 1745–1757.

R Core Team (2018) *R: A Language and Environment for Statistical Computing. Version 3.5.0*. R Foundation for Statistical Computing, Vienna, Austria.

Rensburg, B.J. van, Chown, S.L., & Gaston, K.J. (2002) Species Richness, Environmental Correlates, and Spatial Scale: A Test Using South African Birds. *The American Naturalist*, **159**, 566–577.

Ricklefs, R.E. (1987) Community diversity: relative roles of local and regional processes. *Science, New Series*, **235**, 167–171.

Thuiller, W., Midgley, G.F., Rouget, M., Cowling, R.M., F. Midgley, G., Rougeti, M., & M. Cowling, R. (2006) Predicting patterns of plant species richness in megadiverse South Africa. *Ecography*, **29**, 733–744.

Verboom, G.A., Stock, W.D., & Cramer, M.D. (2017) Specialization to extremely low-nutrient soils limits the nutritional adaptability of plant lineages. *The American Naturalist*, **In press**.

Wardell-Johnson, G. & Horwitz, P. (1996) Conserving biodiversity and the recognition of heterogeneity in ancient landscapes: a case study from south-western Australia. *Forest Ecology and Management*, **85**, 219–238.

654 **Biosketches**

655 **Ruan van Mazijk** is a Masters student interested in phylogenetic systematics, macro-ecology, comparative
656 work and plant functional ecology.

657 **Michael D. Cramer**

658 **G. Anthony Verboom**

659 **Author contributions**

660 MDC and GAV conceived the study question, which RVM investigated under their supervision for his BSc
661 Hons project. The analyses and programming work were largely devised by RVM, with input from the other
662 authors, and was carried out by RVM. RVM wrote the first draft of the manuscript and all authors contributed
663 equally thereafter.

Table 1: Georeferenced vascular plant species occurrence and environmental data sources used in this study. Data were acquired for the Cape and SWA regions, with the temporal extent of data products used described where applicable. Abbreviations are as follows: MAP, mean annual precipitation; PDQ, precipitation in the driest quarter; CEC, cation exchange capacity.

Variable	Source	Temporal extent	Citation
Plant species occurrences	GBIF	TODO	??, ??
Elevation	SRTM v2.0		??
NDVI	MODIS (MOD13C2)	Feb. 2000 to Apr. 2017	??
Climatic variables			
Surface temperature	MODIS (MOD11C3)	Feb. 2000 to Apr. 2017	??
MAP	CHIRPS v2.0	Jan. 1981 to Feb. 2017	??
PDQ	CHIRPS v2.0	Jan. 1981 to Feb. 2017	??
Soil variables			
CEC	SoilGrids250m (CECSOL M 250m)		??
Clay	SoilGrids250m (CLYPPT M 250m)		
Soil C	SoilGrids250m (OCDENS M 250m)		
pH	SoilGrids250m (PHIKCL M 250m)		

Table 2: Average percentile-ranks for BRT-model performance measures (nt , R^2_{pseudo} (Equation (4)), R^2_{E-O}) of 1000 replicate BRT-models relative to 999 BRT-models fit to permuted datasets. Ranks approaching one indicate that a set of replicate BRT-models had greater values than the permuted models.

Model	nt	R^2_{pseudo}	R^2_{E-O}
QDS-richness			
GCFR	1.000	1.000	1.000
SWAFR	1.000	1.000	1.000
HDS-richness			
GCFR	0.987	1.000	0.988
SWAFR	1.000	1.000	1.000
HDS-turnover			
GCFR	0.977	0.992	0.979
SWAFR	0.997	1.000	1.000

Table 3: Estimated differences between replicate Cape and SWA BRT-models' performance measures (nt , R^2_{pseudo} (Equation (4)), R^2_{E-O}) following t -tests. Positive values indicate that the Cape models had greater values. In all cases, the Cape and SWA had highly significantly different values for these quality measures ($P < 0.0001$).

Model	nt	R^2_{pseudo}	R^2_{E-O}
QDS-richness	542.938	0.063	-0.005
HDS-richness	-808.994	-0.064	-0.233
HDS-turnover	-997.045	-0.052	-0.296

665 Figures

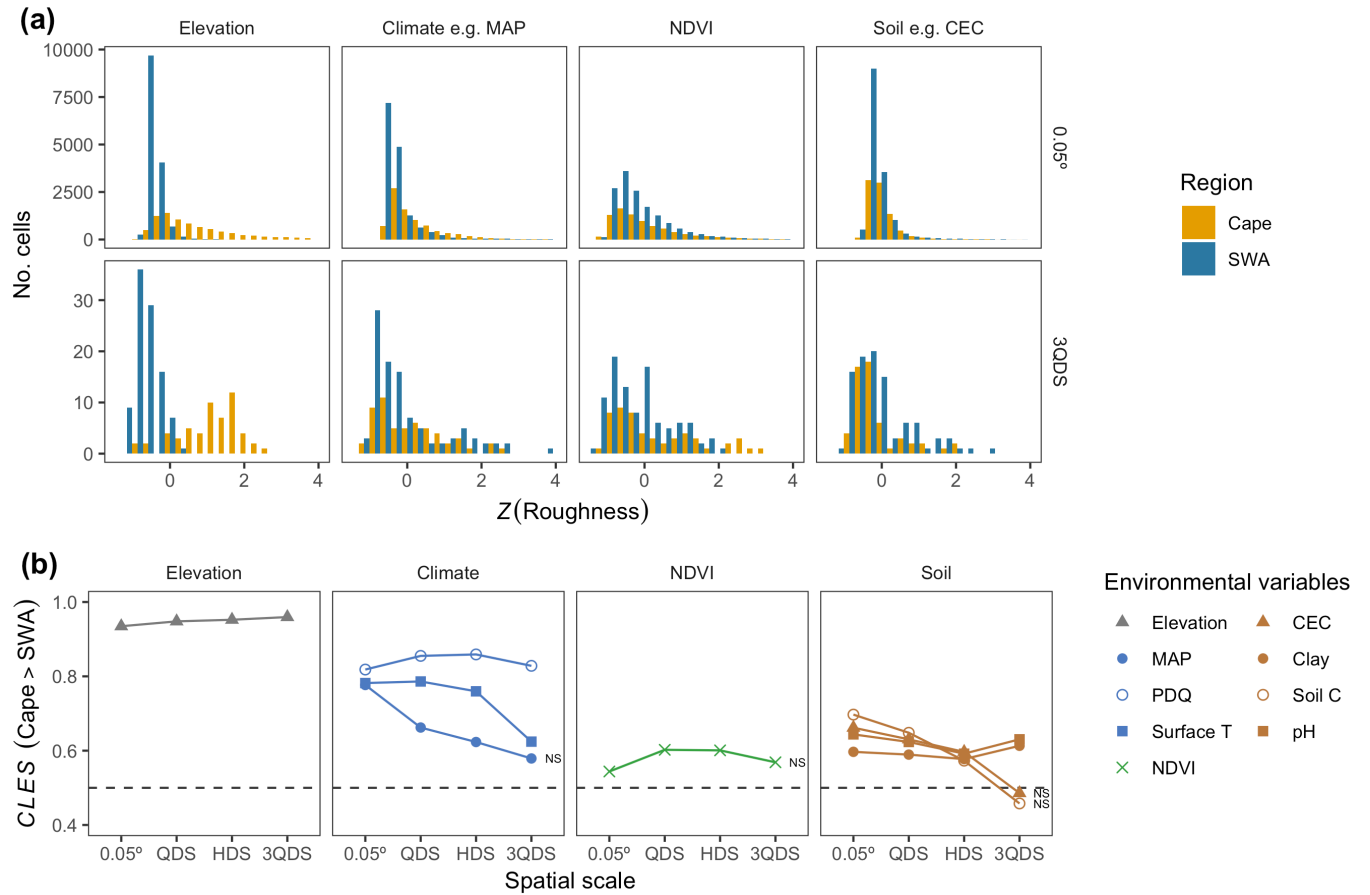


Figure 1: Types of environmental heterogeneity, compared between the the Cape and SWA—namely for (a) elevation, (b) climatic variables, (c) NDVI and (d) soil variables—in each panel consisting of three sub-panels per variable type. The upper row of panels shows example distributions of roughness values (Equation (1)), showing the different extremes in environmental heterogeneity observed in each region when compared at fine (0.05°) and coarse (3QDS) scales. Each distribution has under it an area of one. Histograms were constructed using 20 breaks. In the lower row of panels, these distributions of roughness values were compared between the Cape and SWA at each of the four spatial scales, not just 0.05° and 3QDS, using non-parametric Mann-Whitney U -tests to test for differences. The “common language effect size” ($CLES$, see text) describes these differences (b). U -tests for almost all environmental variables yielded significant differences ($P < 0.05$) between Cape and SWA values (NS, non-significant differences). $CLES$ for 0.05 res. is for 5000 random cells in each region, as the Mann-Whitney U -test cannot handle more than a few thousand values per sample when comparing.

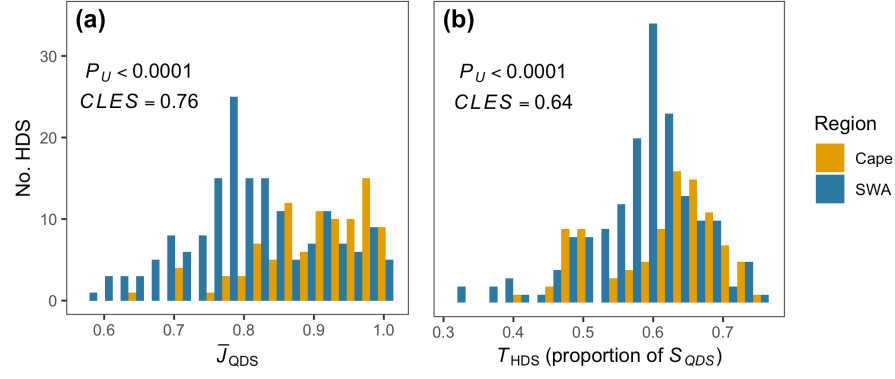


Figure 2: Species turnover, described in two forms ((a) mean Jaccard distance between QDS in each HDS (\bar{J}_{QDS}), (b) additively defined turnover (T_{HDS} , Equation (2)) as a proportion of HDS richness (S_{HDS})), compared between the Cape and SWA. Mann-Whitney U -tests between the Cape and SWA distributions of \bar{J}_{QDS} and T_{HDS} yielded significant differences.

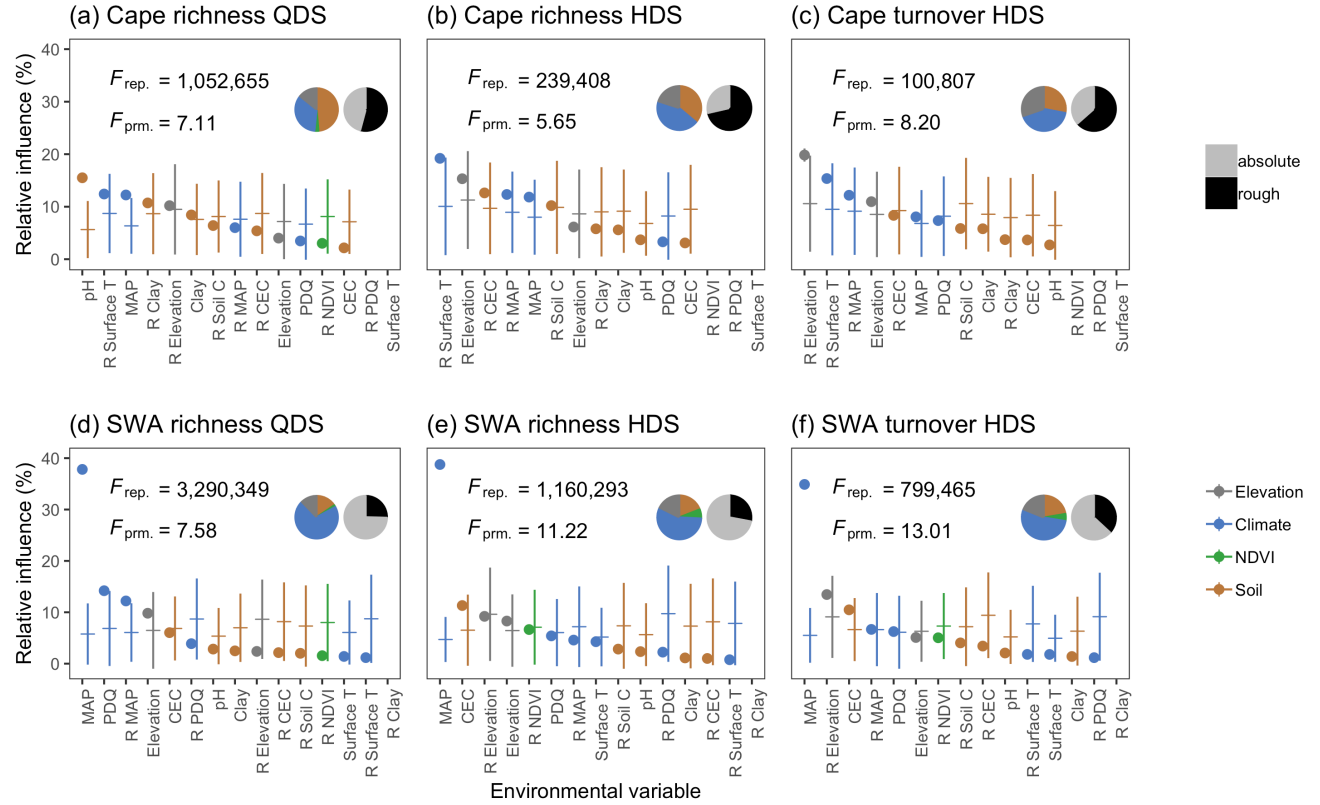
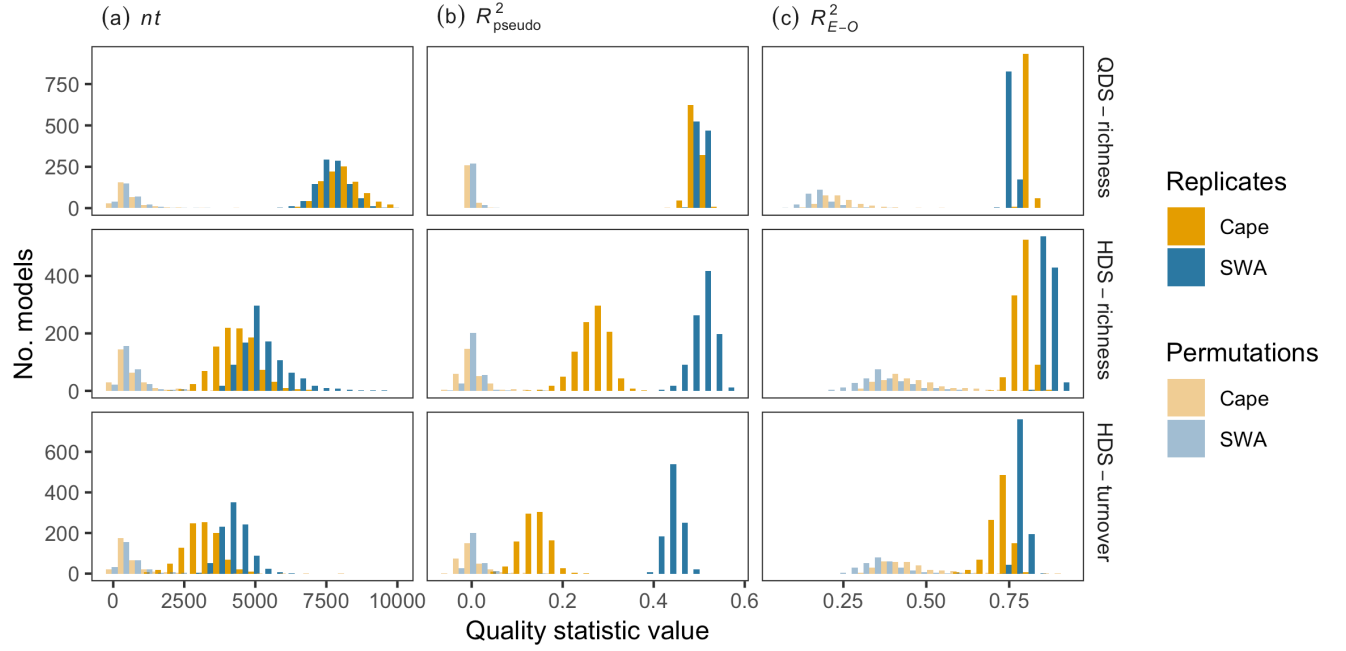


Figure 3: Relative influence of environmental variables (including heterogeneity variables—prefixed with “R”) in boosted regression tree (BRT) model predictions for the final six models’ response variables in the Greater Cape Floristic Region (Cape) and the Southwest Australia Floristic Region (SWA): vascular plant species richness at the (b,e) QDS-scale, (a,d) HDS-scale and (c,f) turnover ($= \bar{J}_{QDS}$). All BRT-models were permitted to fit three-way interactions between environmental variables. Points denote the average contribution of an environmental variable to model-predictions across the 1000 replicate BRT-models for that region/scope. Horizontal ticks denote the average for the 999 permuted BRT-models. The standard deviations above and below these means are shown with vertical lines. Note that in the case of the replicate models they are very small in most cases, obscuring them. Colour represents the general category of the environment (keyed) to which a variable belongs, as in Figure 1b. Piecharts inset display the same information (left-most piecharts), and additionally grouped according to whether a variable was absolute or roughness-transformed (right-most piecharts). F -statistics inset are for one-way ANOVAs of differences in variables’ relative influences from the replicate ($F_{rep.}$) and permuted ($F_{prm.}$) BRT-models.



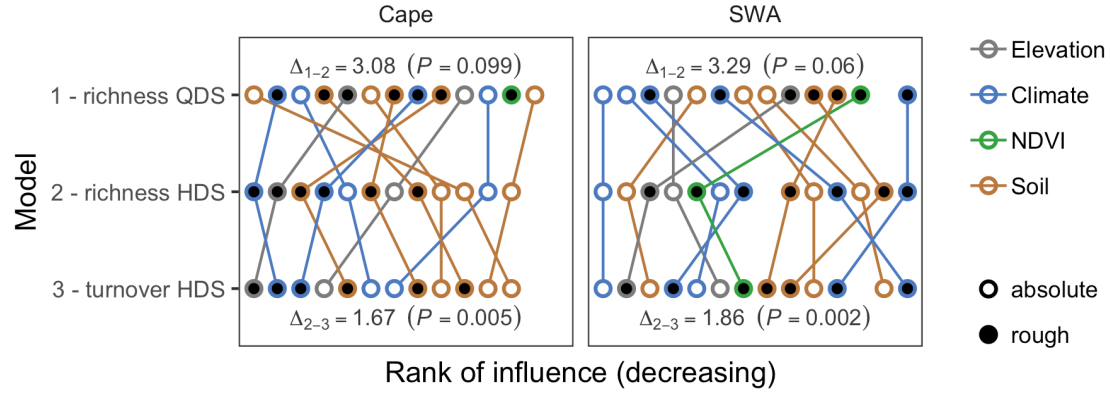


Figure 5: Differences in the rankings of environmental variables' (including heterogeneity variables) relative influences on boosted regression tree (BRT) model predictions of vascular plant species richness and turnover in (a) Cape and (b) SWA (as in Figure 3). Each point represents an environmental variable's rank in BRT-model importance, decreasing in importance from left to right. Rankings used here are the same as that of the average relative influence for variables across replicate BRT-models, presented in Figure 3. Coloured lines connect points representing the same environmental variable. Points' outlines are coloured according to the general category of the environment (keyed) to which a variable belongs, as in Figures 1b and 3, while points' centres are coloured according to whether a variable was roughness-transformed or not. The comparisons of variables' rankings of interest are between QDS- and HDS-scale richness (rows nos. 1 and 2) and between HDS-scale richness and turnover (rows nos. 2 and 3). Statistics (Δ - and P -values) inset at the top and bottom of each panel refer to these comparisons respectively. Δ -values represent the average absolute difference in ranks across variables between two models' rankings. The associate P -value results from ranking the observed Δ -values against 999 Δ -values based on random permutations of variables' rankings (SI1), such that more significant P -values denote rankings more similar than would be expected by chance.

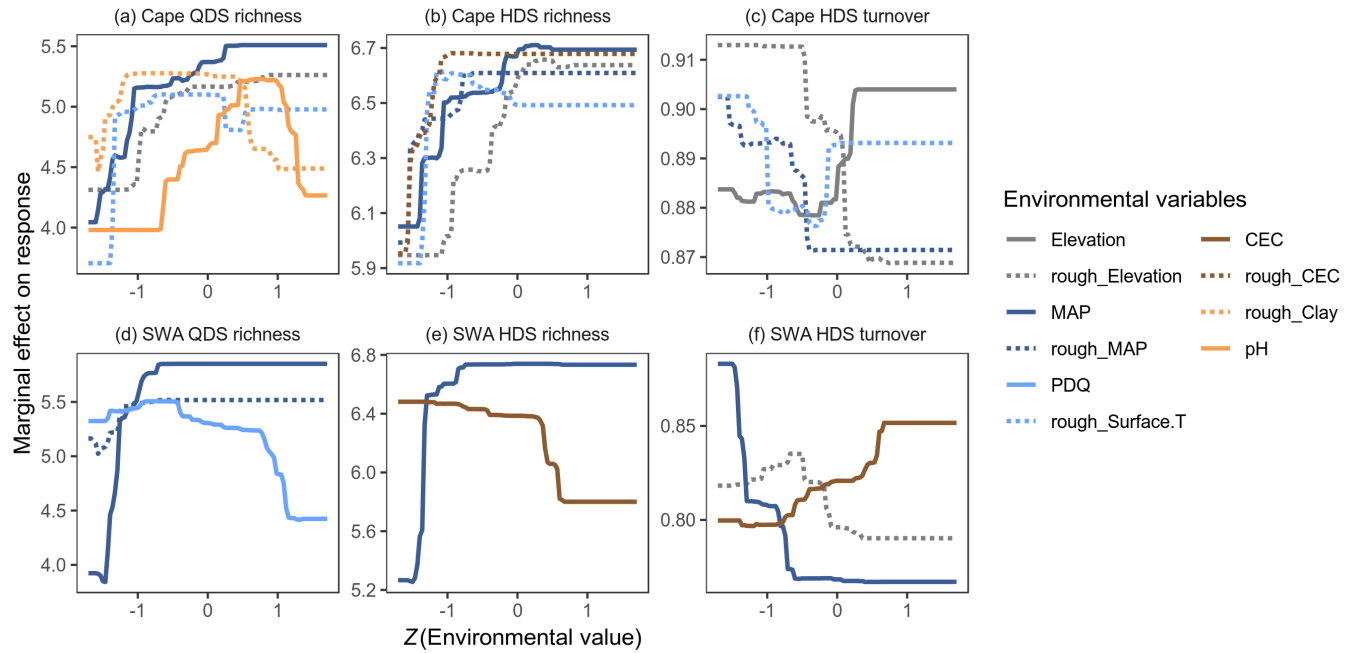


Figure 6: Marginal effects of environmental conditions and heterogeneity on vascular plant species richness at the QDS-scale (a, d), HDS-scale (b, e) and turnover ($= \bar{J}_{QDS}$; c, f) in response variables in the Greater Cape Floristic Region (Cape; a–c) and Southwest Australia Floristic Region (SWA; d–f) following boosted regression tree (BRT) modelling. Marginal effect functions presented are derived from arepresentative BRT-model from the set of replicate BRT-models (for each of the six modelling cases) (see SI regarding how representative BRT-models were selected). Marginal effect functions are shown for environmental variables that contributed $\geq 10\%$ to a model’s predictions. Functions are coloured as keyed, with solid lines representing absolute environmental variables and dotted representing heterogeneity variables (“rough”). Environmental variables were all rescaled here such as to be centred on zero facilitating comparison of functions’ forms.